ARTICLE

Enantioselective Separation Using Chiral Mesoporous Spherical Silica Prepared by Templating of Chiral Block Copolymers

Pradip Paik,[†] Aharon Gedanken,[†] and Yitzhak Mastai*[,‡]

Kanbar Laboratory for Nanomaterials and Institute of Nanotechnology, Department of Chemistry, Bar-Ilan University, Ramat Gan 52900, Israel

ABSTRACT In this work, we synthesized chiral mesoporous silica (CMS) spheres, which can be used as a potential candidate for chiral separation. The CMS spheres with controllable pore sizes (of 2−3 nm) and high surface areas of ca. 614 $m^2 g^{-1}$ were synthesized by chiral templating with chiral block copolymers based on poly(ethylene oxide) and DL-glutamic acid [PEO_{113}-*b*-$(GluA)_{10}$]. The ordered structure of the chiral mesopores was characterized by high-resolution transmission electron microscopy, and the average pore diameters of chiral mesopores were estimated from the nitrogen adsorption−desorption measurements. The enantioselectivity properties and chiral resolution kinetics of the mesopores of silica spheres, after extraction of chiral polymers of PEO_{113}-*b*-$(L/D\text{-}GluA)_{10}$, were scrutinized using a racemic solution of valine and measuring the circular dichroism and optical polarimetery. A chiral selectivity factor of 5.22 was found with a specific enantiomer of valine adsorbed preferably. These results raise the new possibilities of CMS spheres for enantiomeric separation and other enantioselective applications.

KEYWORDS: chiral mesopores • silica spheres • chiral block copolymers • enantiomeric separation

INTRODUCTION

The enantiomeric pure compounds have attracted great technological interest since Pasteur first separated the chiral crystals of tartrate salt in 1848 (1). Essentially chiral materials are of interest for scientific and economic reasons (2). Achieving novel enantiomerically pure compounds is very difficult for its uses, predominantly for pharmaceuticals, agrochemicals, and flavors (3). Most synthesis methods of chiral materials reported so far are based on the asymmetric synthesis where the starting materials are chiral or enantiomerically pure compounds that can be achieved by the chiral resolution of enantiomers. Asymmetric synthesis (4) is, in principle, the most cost-effective method for producing a single isomer. In spite of the noticeable advantages of the asymmetric synthesis, this method has an obvious limitation; e.g., it gives high enantiomeric purity only for exceptionally enantioselective reactions. On the basis of physical, chemical, and biological techniques, the resolution of isomers can be accomplished by various processes (5). New chromatographic techniques (6), commonly based on the approach of linking chiral compounds to a solid substrate and using the resultant material to selectively bind one enantiomer, have been developed in recent years. Chiral polymers (7−9) are also used in numerous chiral applications such as nonlinear optical applications (10), chiral separations (11, 12), and molecularly imprinted polymers (MIPs) (13, 14). In our preceding works, we have demonstrated the potential applications of chiral double hydrophilic block copolymers (15) and chiral polymeric microspheres (16, 17) to direct chirality throughout crystallization, particularly for racemic crystals. The chiral polymers are commonly used for the preparation of MIPs. In spite of the fact that molecular imprinting (MI) methods allow materials to be prepared with high affinity and selectivity for a given target molecule, some of these materials' limitations prevent their use in real applications. Such limitations are, for example, extensive nonspecific binding, slow mass transfer, low sample load capacity, and poor recognition in aqueous systems.

The best way to surmount these limitations is to employ MI methods for the preparation of chiral porous materials. The "template-based" approach to the preparation of amorphous, nanoporous silicas is well-recognized and is defined by Brinker et al. (18) as "a central structure about which a network forms in such a way that removal of the template creates a cavity with morphological and/or stereochemical features related to those of the template". Therefore, it is apparent from the definition that extraction of the chiral template results in chiral nanopores. Following the same approach, in 2004, Alvaro et al. (19) prepared an optically active chiral porous material using chiral binaphthyl and tetraethyl orthosilicate (TEOS), which linearly rotate the polarized light. Corma et al. (20) prepared chiral periodic mesoporous organosilica (ChiMO) for catalytic applications and having enantioselectivity.

In addition, there are recent reports on antibody-based bionanotube membranes for enantiomeric drug separation (21). However, to the best of our knowledge, none of these

* Fax: (+) 972-3-7384053. E-mail: mastai@mail.biu.ac.il.
Received for review June 2, 2009 and accepted July 27, 2009
† Kanbar Laboratory for Nanomaterials. E-mail: pradip.paik@gmail.com (P.P.), gedanken@mail.biu.ac.il (A.G.).
‡ Institute of Nanotechnology.
DOI: 10.1021/am9003842

Published on Web 08/10/2009

systems is effective in chiral separation. Very recently, a general method for the chiral imprinting of sol−gel thin films exhibiting enantioselectivity has been developed by Avnir's group. In a series of articles, Avnir et al. (22, 23) showed that template molecules such as propranolol, 2,2,2-trifluoro-1-(9-anthryl) ethanol, 3,4-dihydroxyphenylacetic acid, and tyrosine can be used to prepare a chiral imprint sol−gel matrix. The shape of the chiral matrix is maintained when the template molecule is extracted. Therefore, the porous materials formed are enantiopure; i.e., the cavity left inside the sol−gel films can discriminate between optical enantiomers. For instance, in a sample of an *S*-imprinted propranolol sol−gel thin film, the *S* film recognized (*S*)-propranolol better and the *R*-imprinted film recognized (*R*)-propranolol better with a discrimination ratio of about 1.5. Similarly, TiO_2 thin films imprinted by chiral carboxylic acids have also been reported, and enantioselectivity has been observed (24). A variety of other imprinting approaches for the preparation of chiral porous materials (25−31), including polymers (32) and dendrimers (33), have been studied. Although an array of such interesting and exciting approaches to the chiral synthesis of porous materials and their uses for chiral separation and other applications have been reported, to the best of our knowledge, none of these materials is effective in enantiomeric separation. Much more can still be accomplished.

With respect to a variety of scientific and technological applications (34−37), in the current research work, we illustrate the synthesis and application of well-ordered chiral mesoporous silica (CMS) spheres by chiral block copolymers (CBCs) of a poly(ethylene oxide) (PEO) block and blocks of chiral L/D-glutamic acid [PEO-*b*-(L/D-GluA)$_n$]. Block copolymers, particularly double hydrophilic block copolymers, are a new class of amphiphilic polymers of rapidly increasing importance with unique and fascinating properties, potentially connecting materials science, pharmacy, biochemistry, and polymer science (38−40). Their chemical structure may be adapted for a wide range of applications covering different aspects such as the stabilization of colloids, crystal growth modification, induced micelle formation, and polyelectrolyte complexing toward novel drug-carrier systems. Because the potential of this novel polymer class is still relatively unexplored, it can be expected that more applications will arise because of the possibility of adapting the chemical structure either to the desired substrate in contact with water or to the stimulus for the induction of structural changes. In this paper, we describe the first application of CBCs of glutamic acid as template surfactants for the synthesis of CMS spheres. Furthermore, we demonstrate that CMS spheres could be used for the enantioselective separation of enantiomers and racemic solutions. Purposefully, Fourier transform IR (FTIR), high-resolution transmission electron mmicroscopy (HRTEM), Brunauer−Emmett−Teller (BET), ^{29}Si NMR, optical polarimeter, and circular dichroism (CD) spectroscopy were used to study the structure and morphology, chirality, enantioselectivity, and chiral resolution kinetics of the CMS.

RESULTS AND DISCUSSION

Synthesis of CBCs. In this research work, we prepared CBCs based on a α-methoxy-ω-aminopoly(ethylene glycol) (PEG; M_w = 5000 g mol^{-1}) block and a block of L- or D-glutamic acid. The syntheses of the CBCs were carried out by the previously reported method (38−40). The details of the syntheses for block copolymers are given as Supporting Information. The reaction sequence for the preparation of a chiral block polymer is also shown in Scheme 1. The structural conformations and the information about the molecular weight are appended in the Supporting Information (Figures S1−S7). Briefly, the CBCs of PEG and glutamic acid are synthesized via ring-opening polymerization of the L- or D-glutamic acid 5-benzyl ester *N*-carboxyanhydride (NCA-GluA5BE) monomer with α-methoxy-ω-amino-poly(ethylene glycol). NCA-(L-GluA5BE) or NCA-(D-GluA5BE) is transformed into a microinitiator for the ring-opening polymerization. Thus, a controlled growth of polymer chains from NCA-GluA5BE may be achieved. The CBCs are optically active.

The ^{1}H NMR and FTIR spectra confirmed their structures (Supporting Information). On the basis of the ^{1}H NMR spectrum (Figure S4) of the block copolymer and matrix-assisted laser desorption ionization time-of-flight (MALDI TOF) analysis (Figure S5), the number of amino acid units in the block is calculated and found to be 10−14, and we considered it on an average of 10. From the integral ratio of PEG and the benzyl group, the number of amino acid groups is calculated (Figure S4). The PEG$_{113}$-*b*-(L-GluA)$_{10}$ and PEG$_{113}$-*b*-(D-GluA)$_{10}$ copolymers show a high polydispersity index [PDI = (average M_w)/(average M_n)] of ca. 1.45 (41), mainly due to the broad distribution of the molecular weights of the polypeptide block, compared to the polypeptide prepared by a living polymerization method (42) (PDI = 1.09). This happens because of the already very polydispersed α-methoxy-ω-aminopoly(ethylene glycol) microinitiator (PDI = 1.40). This PDI value is also high compared to the organonickel-based initiating system bipy-Ni(COD) (43) and other transition-metal complexes (44); the NCA polymerizations of block copolymers are much better controlled and produce well-defined polypeptides with PDI < 1.2.

PEG$_{113}$-*b*-(L-GluA)$_{10}$ and PEG$_{113}$-*b*-(D-GluA)$_{10}$ are highly water-soluble up to 0.5 mg mL^{-1}. The CD spectra for the secondary structures of the CBCs of PEG$_{113}$-*b*-(L-GluA)$_{10}$ in aqueous solutions are shown in Figure 1. The CD spectroscopy results demonstrate that the synthetic chiral polymer PEG$_{113}$-*b*-(L-GluA)$_{10}$ can adopt two main types of secondary structures such as an α-helix and a random coil. Moreover, the structure depends on the measurement conditions, mainly on the pH. From our CD spectroscopy results (Figure 1), we found that, at pH = 3.5 and 25 °C, the amino acid block copolymer PEG$_{113}$-*b*-(L-GluA)$_{10}$ shows 83−85% of a α-helix structure identified by the two minima at λ = 208 and 219 nm and 15−17% of a random coil, due to the polydispersity of the block copolymer. The calculations of the α-helix and random coil percentages were performed according to the literature (45, 46). The formation of the micelles of an average

Scheme 1. Synthesis of the Block Copolymer of Poly(ethylene oxide)-L-glutamic Acid [PEO_{113}-*b*-(L-GluA)$_n$], Where $n = 10$

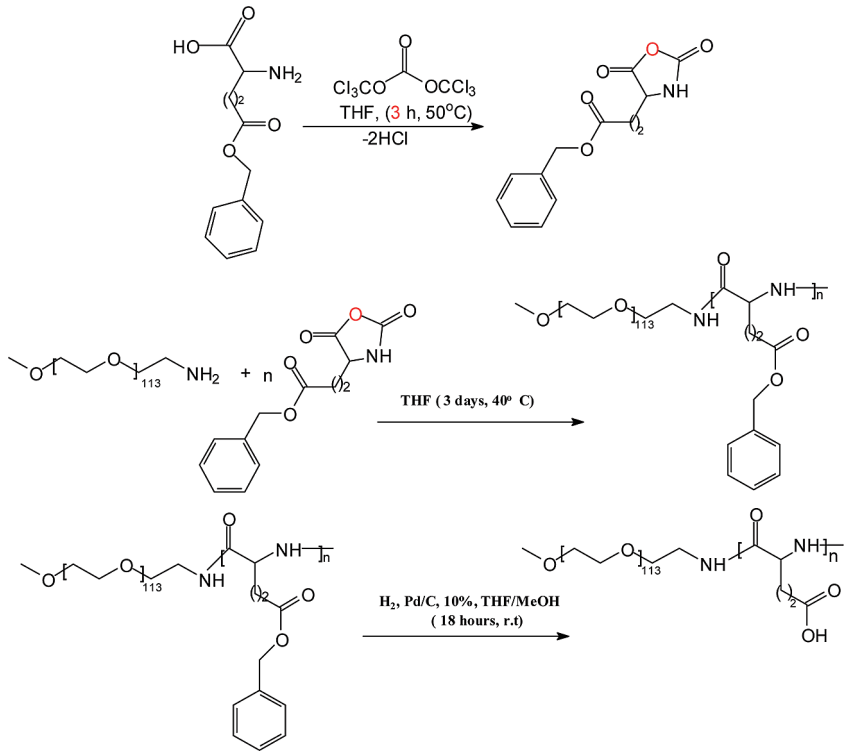

diameter of ca. 10 nm has been observed through dynamic light scattering experiments for the PEG_{113}-*b*-(L-GluA)$_{10}$ copolymer at pH = 3.5 (1.0 mg mL^{-1}) and 25 °C. All of these results corroborate the robustness of our synthetic block copolymers because the analogous results for the structure of a synthetic block copolymer of amino acid match well with the literature (38, 47).

CBC Templating and Synthesis of CMS Spheres. We synthesized the CMS spheres as shown in Figure 2. Our approach for the synthesis of CMS spheres is based on a polymer templating sol−gel method. The details of the synthesis method are explained in the Experimental Section. It has been reported that mesoporous materials can be synthesized with a self-assembled amphiphilic molecules templating route (48−50). It is also well-known that lipid amphiphilic molecules such as amino acids and fatty acids with chiral alkyl hydrophobic chains can self-organize to form a nanostructure material with bilayer molecular arrangement (51, 52). Therefore, the formation of a chiral porous silica began with the templating of helical CBCs, and in this way, the CMS spheres can be synthesized. The self-assembly of CBCs leads to organized chiral mesopores. The preparation method yields a CBC that is found inside the mesoporous structure. This structure has been confirmed by FTIR spectra (Figure 3), nitrogen adsorption−desorption data (Figures 4 and S8 in the Supporting Information), and BET surface area data of the as-synthesized silica spheres (As-SiO_2), without extraction of the CBCs. The same three techniques were also applied to CBC-extracted silica spheres (Ex-SiO_2) after extraction of the CBCs, and they indicated the absence of CBCs inside the CMS. Therefore, the extraction of the CBCs from As-SiO_2 is urgent to get the open chiral pores. The key step performed for this work is to take out the CBCs by solvent extraction for 72 h using chloroform at relatively low temperature, 35 °C. We avoid high temperatures during the solvent extraction process because of the high possibility of denaturizing the imprinted chiral mesostructures because of the solid-state diffusion of the atoms. In Figures S3 and S4 in the Supporting Information, we present the FTIR and ^{1}H NMR results, respectively, of PEG_{113}-*b*-(L-GluA5BE)$_{10}$. It is obvious from the FTIR results (Figure S3 in the Supporting Information) that PEG_{113}-*b*-(L-GluA5BE)$_{10}$ block copolymer shows three main characteristic peaks at 1547 cm^{-1} (amide II, N−H, C−N), 1653 cm^{-1} (amide, C═O), and 1731 cm^{-1} (benzyl ester, C═O). The ^{1}H NMR (300 MHz, $CDCl_3$) results corroborate the results for PEG_{113}-*b*-(L-GluA 5BE)$_{10}$ as well. The FTIR results (Figure S6 in the Supporting Information) for PEG_{113}-*b*-(L-GluA)$_{10}$ show characteristic peaks at 1558 cm^{-1} (amide II, N−H, C−N) and

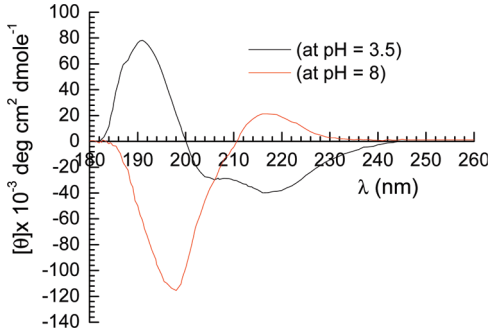

FIGURE 1. CD spectra of CBCs of PEG_{113}-*b*-(L-GluA)$_{10}$ at (A) pH 3.5 and (B) pH 8.

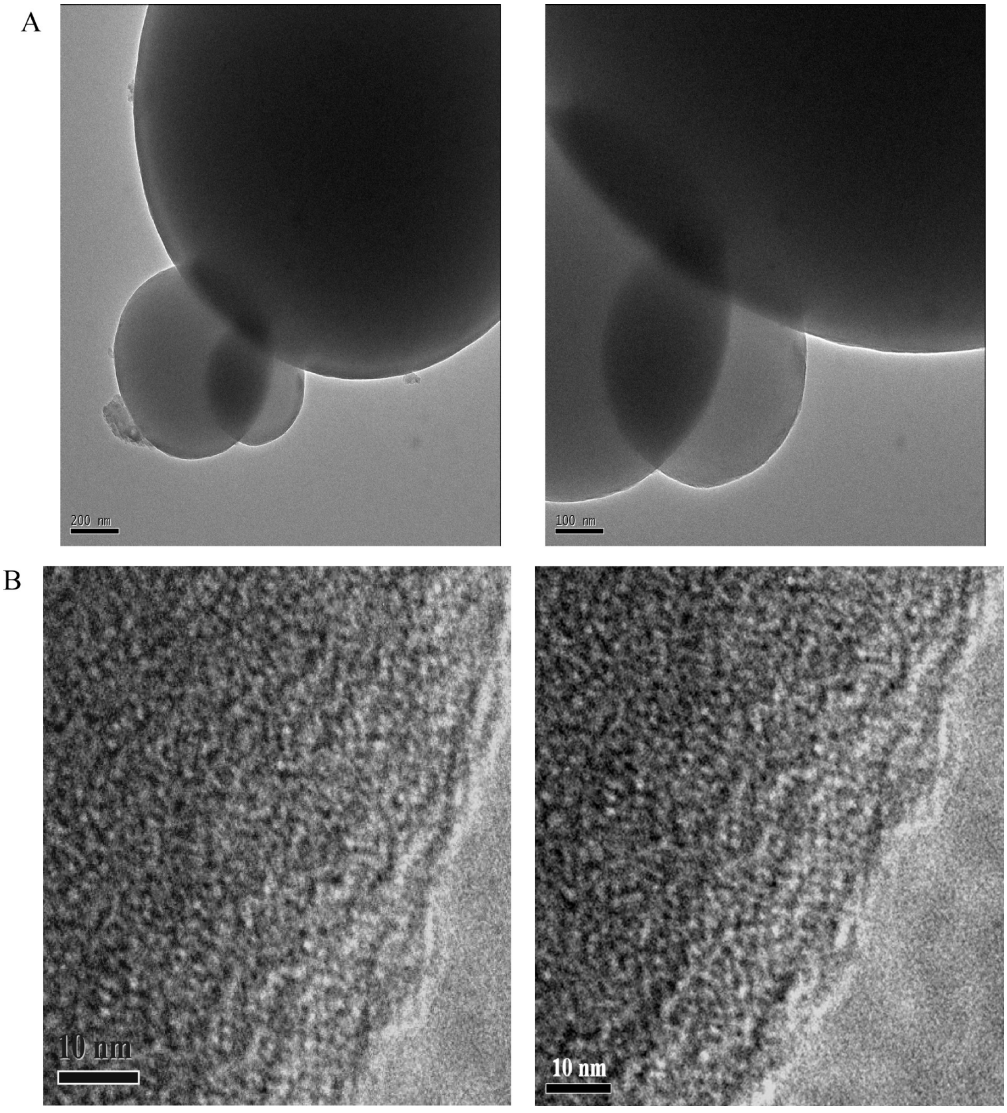

FIGURE 2. HRTEM images: (A) low resolution (B) high resolution of CMS spheres (Ex-SiO_2) synthesized by templating PEG_{113}-*b*-(L-GluA)$_{10}$. The pore size is 2−3 nm.

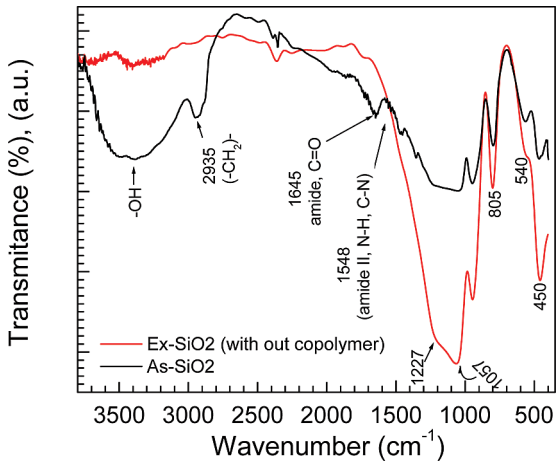

FIGURE 3. FTIR spectra of chiral mesoporous As-SiO_2 and Ex-SiO_2.

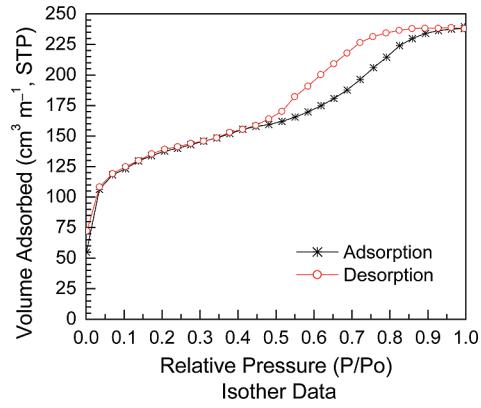

FIGURE 4. Nitrogen adsorption−desorption isotherm (BET) of chiral mesoporous Ex-SiO_2 (BET surface area = 614 m^2 g^{-1}; pore diameter = 2−3 nm).

1659 cm^{-1} (amide, C═O). The ^{1}H NMR (300 MHz, CD_3Cl) (Figure S6 in the Supporting Information) results for PEG_{113}-*b*-(L-GluA)$_{10}$ detect also the presence of the L-GluA group in the CBCs. Thus, both the FTIR and ^{1}H NMR results show the existence of L-GluA in the CBCs. The FTIR results (Figure 3) of As-SiO_2 reveal absorption peaks for the block copolymers at 1548 cm^{-1} (amide II, N−H, C−N), 1645 cm^{-1} (amide, C═O), 2935 cm^{-1} (−CH_2), and 3500 cm^{-1} (−OH), whereas after solvent extraction, these peaks have disappeared

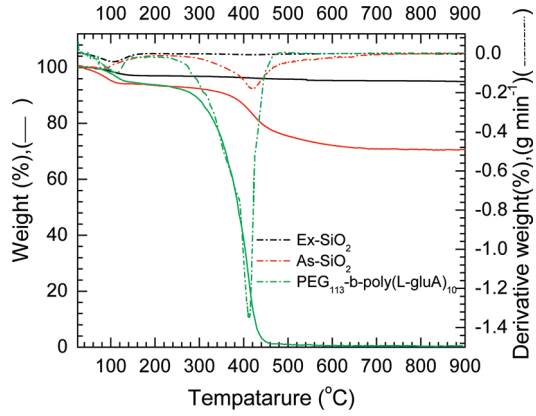

FIGURE 5. TGA of chiral mesoporous Ex-SiO_2, As-SiO_2, and PEG_{113}-*b*-(L-GluA)$_{10}$. The solid lines represent the TGA and the dotted lines the DTGA of corresponding materials with respective colors.

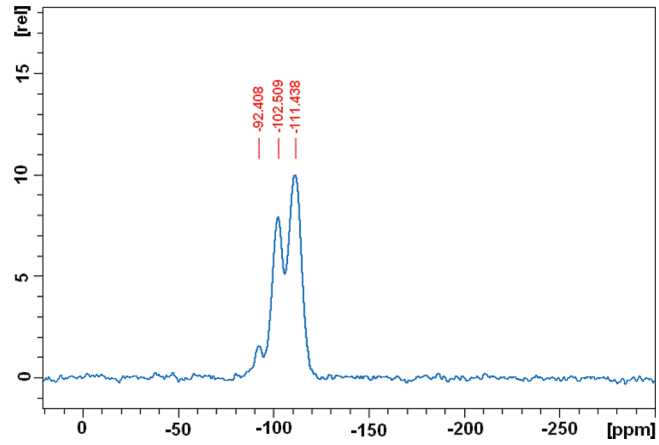

FIGURE 6. Solid-state ^{29}Si NMR spectra of chiral mesoporous Ex-SiO_2. The spectra show peaks at −111.43 ppm (Q^4), −102.50 ppm (Q^3), and −92.40 ppm (Q^2) [$Q^n = Si(OSi)_n(OH)_{4-n}$, $n = 2-4$].

(Figure 3). Therefore, the FTIR results clearly demonstrate that the block copolymers have been removed successfully from the pores of the spherical silica particles and leave open pores.

Further, the removal of the CBCs is substantiated by BET measurements. Nitrogen adsorption−desorption isotherms were measured for the as-prepared (Figure S8 in the Supporting Information) and extracted materials (Figure 4). The nitrogen physisorption isotherm of the chiral mesoporous product (Ex-SiO_2) is shown in Figure 4. The figure reveals a typical type IV isotherm with hysteresis, which is characteristic for mesoporous silica templated by CBCs. Hysteresis is not observed for As-SiO_2 (Figure S8 in the Supporting Information). The specific surface areas of As-SiO_2 and Ex-SiO_2 are 205 and 614 $m^2\ g^{-1}$, respectively. The pore diameter of Ex-SiO_2 is 2−3 nm (Figure S9 in the Supporting Information). This was calculated from the desorption branch of the BET surface area (Figure 4). The average pore diameters of Ex-SiO_2 spheres were also estimated by measuring 10 randomly chosen HRTEM micrographs, and the measured diameters are matching well with the pore sizes obtained from the nitrogen adsorption−desorption data.

In order to ensure the full removal of the CBCs via the solvent-extraction process, thermogravimetric analysis (TGA) experiments were also performed for PEG_{113}-*b*-(L-GluA)$_{10}$, As-SiO_2, and Ex-SiO_2. The TGA and differential TGA (DTGA) plots are shown in Figure 5. The ∼5% weight loss for Ex-SiO_2 is observed around 80−120 °C because of the presence of moisture (H_2O). No other indication of weight loss is observed up to 900 °C that could be attributed to the loss of carbon residues, whereas the overall 25% weight loss for the As-SiO_2 sample is observed between 450 °C as a result of the elimination of PEG_{113}-*b*-(L-GluA)$_{10}$. We have also shown the TGA and DTGA plots for PEG_{113}-*b*-(L-GluA)$_{10}$ in the same figure (Figure 5) as evidence. The elemental analysis measurements for the extracted CMS spheres were performed, and there is no indication to be found for the presence of nitrogen (0.00%) and carbon (ca. 0.5%). Both the TGA/DTGA and elemental analysis experiments prove the complete removal of the chiral CBCs from the mesoporous Ex-SiO_2 spheres.

The sizes of the mesoporous silica particles range from submicrometer to a few hundred nanometers in diameter, and the particles are spherical in shape. The HRTEM micrographs for the chiral mesoporous Ex-SiO_2 are shown in Figure 2. The white parts on HRTEM micrographs can be considered to be the chiral pores of diameter 2−3 nm, which could be created by the templating of CBCs. It is concluded that each of the large submicrometer spheres is aggregated of many small-size (diameter 2−3 nm) particles. The templating effect is also confirmed from the nitrogen adsorption−desorption data of the as-synthesized and extracted silica spheres, as evidenced from the dramatic change in the surface area upon extraction of the CBCs from the mesoporous silica. The BET surface area of Ex-SiO_2 is 614 $m^2\ g^{-1}$, compared to 205 $m^2\ g^{-1}$ for As-SiO_2. The as-synthesized sample has a low surface area because it is packed with CBC templates. The increase in the surface area is due to extraction of the CBC templates.

The connectivity and the structural periodicity (homogeneous chemical and structural surroundings) of the functional organic groups to the silica framework of solvent-extracted CMS spheres are best demonstrated by cross-polarized ^{29}Si MAS NMR spectroscopy (Figure 6). The spectra exhibit the characteristic resonances at their usual spectral positions, at −111.44 ppm (Q^4) and −102.51 ppm (Q^3) [$Q^n = Si(OSi)_n(OH)_{4-n}$, $n = 2-4$], representing the fully condensed silica and silica with one terminal hydroxyl group. The geminal hydroxyls [Q^2, $(SiO)_2Si(OH)_2$] are barely present in the CMS spheres (resonance at −92.41 ppm) compared to Q^4 [siloxane, $(SiO)_4Si$] and Q^3 [single silanol, $(SiO)_3SiOH$]. The absence of additional peaks indicates the successful extraction of CBCs from the CMS spheres.

In summary, we conclude that the CBCs are effective for the preparation of CMS spheres. The mesopores are highly ordered, periodically mesoporous structures with pore sizes of ca. 2−3 nm and specific surface areas of 614 $m^2\ g^{-1}$. The CMS spheres are obtained under acidic conditions using a CBC as a supramolecular structure-directing agent.

Chiral Recognition, Enantioselective Separation, and Chiral Resolution Kinetics. In the next stage, we

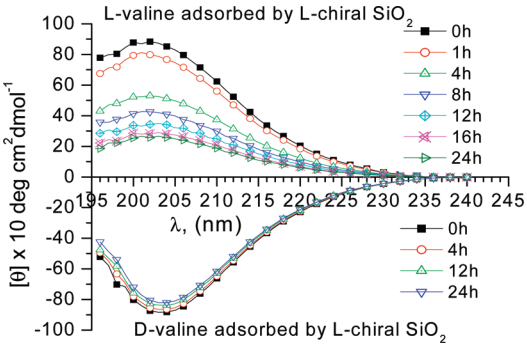

FIGURE 7. CD spectra of L- and D-valine into the L-imprinted mesoporous chiral Ex-SiO_2.

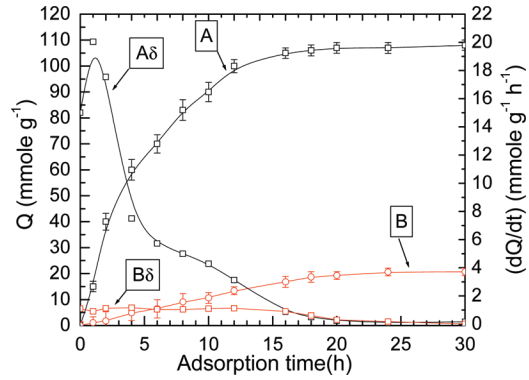

FIGURE 8. Curve of adsorption dynamics (Q vs t) from a solution of valine enantiomers into the mesoporous chiral Ex-SiO_2: (A) D-valine; (B) L-valine. Curve of the derivative of adsorption dynamics (dQ/dt) vs t: D-valine (Aδ); L-valine (Bδ).

examined the chiral recognition ability of our CMS spheres. We chose DL-valine, a small chiral molecule, as a representative case to demonstrate the chiral recognition ability of the mesoporous silica. DL-Valine was used in order to probe the specific chiral interactions with the surface chirality of the imprinted mesoporous silica due to the similarity of the valine, in terms of polarity, hydrophobicity, and acidity, to the chiral template molecule. In general, chiral binding and selectivity of enantiomers to CMS can be tested with various analytical tools such as fluorescence analysis and isothermal titration calorimetry (53−55).

In this work, we selected CD spectroscopy as the method for exploring the chiral recognition of our CMS spheres. We performed selective chiral adsorption measurements of enantiomers and also of racemic solutions of valine. The evaluation of the amount of adsorbed molecules onto the CMS spheres was determined by CD spectroscopy. Adsorption measurements were carried out by taking aqueous solutions of 150 mM L or D enantiomer of valine. This amount of each enantiomer was added to the chiral imprinted silica, and their optical activities were measured with time. For both solutions, 2 mg of CMS prepared from PEG_{113}-*b*-(L-$GluA)_{10}$ (after CBC extraction) was added to 1 mL of the standard 150 mM L- or D-valine. The CD of the solutions was probed as a function of time. The CD spectra of the valine enantiomers are shown in Figure 7. As is seen from Figure 7, the ellipticity (deg cm^2 $dmol^{-1}$) of the CD band for L-valine decreased rapidly during the first 3 h, and in the second stage (4−12 h), it decreased but not at the same speed. The intensity of the CD band remains unchanged between 16 and 24 h. Similar types of experiments were performed with the extracted CMS spheres synthesized by templating PEG_{113}-*b*-(L-$GluA)_{10}$ to study the adsorption of D-valine in the same experimental conditions. From Figure 7, we found that the intensity of the CD band for D-valine remained unchanged with time. This means the amount of D-valine adsorbed by the CMS synthesized by templating PEG_{113}-*b*-(L-$GluA)_{10}$ is negligible and the rate of absorption is very slow. A comparison of the adsorption of L and D enantiomers of the CMS spheres synthesized by templating PEG_{113}-*b*-(D-$GluA)_{10}$ is also shown (Figure S10 in the Supporting Information). We found that the preferable D-valine is adsorbed by the CMS synthesized by templating PEG_{113}-*b*-(D-$GluA)_{10}$ and the amount of adsorption of L-valine is negligible. The representative plots of adsorption dynamics (Q vs t) and kinetics (dQ/dt vs time) of L-valine for the extracted silica sphere synthesized by templating PEG_{113}-*b*-(L-$GluA)_{10}$ obtained from optical polarimetry experiments are shown in Figure 8. As can be seen from Figure 8, the amount of the adsorbed valine Q (mmol g^{-1} of the chiral silica) increases rapidly during the first 3 h for both enantiomers. In the second stage (4−12 h), the rate of adsorption decreases progressively and reaches a maximum value at 18 h. These results clearly demonstrate the stereoselective uptake of D/L enantiomers by the chiral silica, which displays a significant difference in the adsorption kinetics of the enantiomers. For example, after 4 h, approximately 60 mmol of L-valine was adsorbed, while at the same time, 5 mmol of D-valine was adsorbed. Therefore, it is obvious that the CMS synthesized by templating PEG_{113}-*b*-(L-$GluA)_{10}$ recognizes L-valine better than D-valine. A similar trend is observed for the CMS synthesized by templating by PEG_{113}-*b*-(L-$GluA)_{10}$. Consequently, on the basis of the equilibrium concentrations of L and D enantiomers, an equilibrium discrimination ratio of 5.22 is calculated. This enantioselectivity value is adequate for carrying out successful enantiomeric separation (56, 57).

In a similar approach, we also performed chiral adsorption measurements of alanine enantiomers onto the chiral silica. The adsorption kinetics and the chiral resolution factor of alanine enantiomers are very similar to those of valine. For alanine, an equilibrium discrimination ratio of 4.85 and an enantiomeric excess (ee) of 48% are calculated. From the above results of the adsorption measurements on chiral silica, we can illustrate two important conclusions. First, the templated cavity is able to recognize the chirality of various amino acids having a chirality different from that of the templating molecules and, second, the chiral imprinted silica also adsorbs specific enantiomers with the same chirality as the templated molecule compared to the enantiomers with a chirality opposite to that of the templated molecule, although the nonspecific adsorption is much lower in comparison to chiral-specific adsorption. Because of the amorphous nature of the silica, all of the binding sites may not be identical in nature and, for instance, there may be domains with different accessibilities as well as nonchiral sites. In addition, the formation of nonchiral sites can result from the incompleteness of the silica monomer−chiral

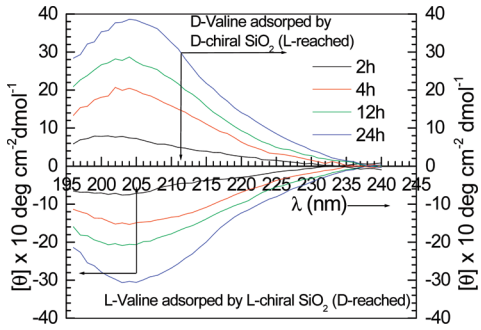

FIGURE 9. CD spectrum of a DL-valine racemic mixture with CMS as a function of time.

template association. It is obvious that some amount of the silica monomer is not associated with the chiral template, and as a consequence, only part of the chiral template added to the silica monomer mixture gives rise to selective chiral binding sites. It should be mentioned that the chiral silica preparation is different from that of the covalent chiral imprinting of polymers, where, theoretically, all of the template sites should be associated with a templated binding site. In general, the existence of nonchiral sites can explain the minute adsorption of valine and alanine enantiomers with the opposite chirality of the templated CBCs.

Finally, we performed chiral adsorption measurements of racemic solutions of valine to demonstrate the chiral resolution capability of the mesoporous silica. Solutions of 150 mM racemic (DL) valine and 2 mg mL^{-1} of chiral silica were mixed together, and the optical activity of the solution as a function of time was measured. The results of those experiments are shown in Figure 9. Analyses of the CD spectra verify the high chiral discrimination of the chiral silica. The ee (%) of the solution increases with time, and at equilibrium, an ee of about 50% of the L enantiomer in solution is achieved when PEG_{113}-*b*-(D-GluA)$_{10}$ imprinted CMS was taken under study. This proves that solid CMS is enriched with the L enantiomer, meaning that the D enantiomer is preferentially absorbed to the CMS. However, in spite of the high ee for valine of ca. ~50% observed in our CMS, the kinetics of the molecular recognition process is slow. For example, after 1 h, a very low value of ee (~10%) is detected, and the maximum ee is attained after 18 h. However, the reason for the slow adsorption kinetics is not clear to us. For most applications of specific molecular recognition, rapid chiral resolution kinetics is essential. Further studies are ongoing in order to make the recognition kinetics faster, which will have a significant impact on the performance of our chiral silica and for its use in chiral separation techniques.

CONCLUSIONS

In conclusion, the impact of chirality on almost any chemical and biological process is well-recognized and has significant ramifications in many fields of economic interest. Because of the increasing demand for enantiomerically pure compounds, efficient strategies for analytical and preparative separations of enantiomers are required. A number of new chiral separations based on the use of chiral porous silica materials have appeared in the field of chiral technology. In this work, we have described a method for the preparation of CMS spheres and demonstrated their enantioselectivity property in the resolution of racemic solutions. We showed that CBCs based on a PEO block and poly(glutamic acid) are good surfactant templates for the fabrication of chiral mesoporous materials with high surface areas as well as narrow pore size distributions. CMS has shown high enantioselectivity after extraction of the chiral copolymers, examined by the selective adsorption of valine enantiomers. The chiral resolution of a valine racemic solution was measured by CD spectroscopy as well as by optical polarimetry, and a high ee of ca. 50% valine was found. It is evident that, besides the very high surface area, high capacity, and technical accessibility of these chiral materials, they should also exhibit higher mechanical and thermal stabilities than the MIPs and therefore could be used as stationary phases in chromatography. Therefore, it is obvious that in the future a variety of pure chiral materials can be separated from a recimic mixcture using this CMS.

EXPERIMENTAL SECTION

Materials. Triphosgene (Aldrich), L/D-glutamic acid 5-benzyl ester (Sigma), and α-methoxy-ω-aminopoly(ethylene glycol) (Iris Biotech GmbH, Marktredwitz, Germany) were purchased and used as received without further purification. The block copolymer of PEG and L/D-glutamic acid was synthesized according to the previous report (38−40).

Synthesis of NCAs of L- or D-Glutamic Acid γ-Benzyl Ester. A solution of triphosgene (1.246 g, 0.0042 mol) in 20 mL of THF was added to a suspension of L-glutamic acid 5-benzyl ester (2 g, 0.0084 mol) in 20 mL of THF. The mixture was stirred for 3 h at 50 °C under an argon atmosphere. After 1 h, suspensions became a transparent solution. The solvent was evaporated under reduced pressure. The product was crystallized from THF/*n*-hexane. Crystalline product was dissolved in 30 mL of cold ethyl acetate and washed by a cold solution of sodium bicarbonate in water (0.5%, 100 mL). The layer of ethyl acetate was isolated, and the solvent was evaporated under reduced pressure. The product was recrystallized three times from a mixture of THF/*n*-hexane and dried at room temperature in vacuum. The yield of NCA of glutamic acid γ-benzyl ester is 1.8 g (82%).

Synthesis of Copolymer Poly(ethylene oxide)-*block*-poly(L-glutamic acid γ-benzyl ester). A solution of the NCA of glutamic acid 5-benzyl ester (0.8 g, 0.0015 mol) in 10 mL of THF was added to a solution of α-methoxy-ω-aminopoly(ethylene glycol) (1 g, 0.0001 mol; M_w = 5000 g mol^{-1}) in 20 mL of THF. The mixture was stirred over 3 days at 40 °C under an argon atmosphere. Then the solvent was evaporated under reduced pressure, and the product was dissolved in 5 mL of THF and precipitated in petroleum ether (or *n*-hexane). The yield was 1.3 g.

Deprotection of the γ-Carboxylic Group of Glutamic Acid. *Catalytic Hydrogenation.* For catalytic hydrogenation, palladium on charcoal (10% Pd/C) was used as a catalyst. The polymer (1 g) was dissolved in 80 mL of 1:1 THF/methanol, and 0.4 g of catalyst was added. The mixture was charged with hydrogen and stirred for 24 h at room temperature. The catalyst was removed by filtration. The solvent was evaporated under reduced pressure. The product was dissolved in water, dialyzed (against pure water for 3 days), and freeze-dried.

Preparation of Spherical CMS. Spherical CMS was synthesized using a chiral surfactant based on CBCs of chiral glutamic acid and PEG as the template and TEOS as the precursor for

silica. In a typical synthesis, [PEO_{113}-*b*-$(GluA)_{10}$] (1 mmol) was dissolved in deionized water (32 g) and stirred at room temperature. HCl (0.1 M, 0.14 mmol) was added to the CBC solution under vigorous stirring at room temperature. After the mixture was stirred for 1 h, 1.4 g of TEOS (0.14 mmol) was added to the solution and the mixture was stirred at 40 °C for 6 h. The mixture was allowed to react at 40 °C under static conditions for 18 h. The chiral mesostructured product thus formed was cured at 80 °C for an additional 24 h. The product was recovered by centrifugal separation and dried under vacuum. The extraction process for the removal of the CBCs was carried out by stirring the as-prepared material in chloroform repeatedly for 48 h at 35 °C. The solid material was washed three times with water, recovered by centrifugal separation, and dried under vacuum. The HRTEM and SEM images of the CMS spheres are shown in Figures 2 and S11 in the Supporting Information.

HRTEM. HRTEM images were acquired with a JEOL JEM-2100 electron microscope using an accelerated voltage of 200 kV.

FTIR Spectroscopy. The FTIR spectra were recorded with a Varian spectrophotometer at room temperature with KBr pellets.

BET Surface Area Analysis. The surface area was measured at 77 K (liquid nitrogen) on a Micromeritics instrument (Gemini 2375) after the samples had been evacuated at 120 °C for 12 h with an evacuator (Micromeritics Flow Prep 060). From the adsorption isotherm, the Barrett–Joyner–Halenda theory was used to calculate the mesopore volume and its size distribution.

^{1}H NMR Spectroscopy. The ^{1}H NMR spectra for the CBC were recorded by a Bruker DZH 300/54, 300 MHz spectrometer.

^{29}Si NMR Spectroscopy. The solid-state ^{29}Si NMR spectra were measured for mesoporous silica spheres by a Bruker 5000 UltraShield spectrometer.

CD Spectroscopy. CD measurements were carried out with a Jasco J-715 spectrometer (model 6025) using a cylindrical quartz cell (1 mL) at 25 °C.

TGA. TGA measurements were performed with a ThermoONIX Gaslab 300 TGA instrument.

Light scattering measurements of the block copolymers were performed at room temperature with a Coulter N4Plus dynamic light scattering instrument.

MALDI TOF Spectroscopy. The molecular weights of the CBCs were confirmed by MALDI TOF spectroscopy (Bruker Autoflex III Smartbeam).

Acknowledgment. The work was supported by the Israel Science Foundation, Government of Israel. This research was supported by the Israel Science Foundation (ISF) grant no. 660/07. The experimental facilities are available in the Institute of Nanotechnology, Department of Chemistry, Bar-Ilan University, Israel.

Supporting Information Available: FTIR and H^1 NMR spectra of NCA-L-Glu5BE (Figures S1 and S2), PEG_{45}-*b*-poly(L-$Glu5BE)_{10}$ (Figures S3 and S4), and PEG_{45}-*b*-poly$(GluA)_{10}$ (Figures S6 and S7), MALDI TOF spectra of PEG_{45}-*b*-poly$(Glu5BE)_{10}$ (Figure S5), nitrogen adsorption–desorption isotherm of As-SiO_2 (Figure S8), nitrogen adsorption–desorption isotherm pore size distribution of Es-SiO_2 (Figure S9), CD adsorption spectra of D- and L-valine of D-chiral imprinted CMS with time (Figure S10), SEM micrograph of chiral mesoporous Ex-SiO_2 (Figure S11), CD adsorption spectra of DL-alanine solution with time (Figure S12), and CD adsorption dynamics for DL-alanine (Figure S13). This material is available free of charge via the Internet at http://pubs.acs.org.

REFERENCES AND NOTES

(1) Pasteur, L. C. R. *Acad. Sci. Paris* **1848**, *26*, 535–538.
(2) Maier, N. M.; Franco, P.; Lindner, W. *J. Chromatogr. A* **2001**, *906*, 3–33.
(3) Dieguez, M.; Pamies, O. P.; Claver, C. *Chem. Rev.* **2004**, *104*, 3189–3215.
(4) Procter, G. *Asymmetric Synthesis*; Oxford University Press: New York, 1997; pp 1–248.
(5) Wilson, I.; Poole, C.; Cooke, M. *Encyclopedia of Separation Science*; Academic Press: London, 2000; Vols. 1–*10*.
(6) Franco Minguillón, C. *Chiral Separation Techniques: A Practical Approach*; Wiley-VCH: New York, 2006; pp 29–559.
(7) Nakano, T. *J. Chromatogr., A* **2001**, *906*, 205–225.
(8) Okamoto, Y. *Prog. Polym. Sci.* **2000**, *25*, 159–162.
(9) Itsuno, S. *Prog. Polym. Sci.* **2005**, *30*, 540–558.
(10) Wulff, G.; Zweering, U. *Chem.—Eur. J.* **1999**, *5*, 1898–194.
(11) Yamamoto, C.; Okamoto, Y. *Bull. Chem. Soc. Jpn.* **2004**, *77*, 227–257.
(12) Zhang, K.; Krishnaswami, R.; Sun, L. *Anal. Chim. Acta* **2003**, *496*, 185–193.
(13) Wulff, G. *Angew. Chem., Int. Ed. Engl.* **1995**, *34*, 1812–1832.
(14) Takeuchi, T.; Haginaka, J. *J. Chromatogr., B: Anal. Technol. Biomed. Life Sci.* **1999**, *728*, 1–20.
(15) Mastai, Y.; Sedlak, M.; Colfen, H.; Antonietti, M. *Chem.—Eur. J.* **2002**, *8*, 2430–2437.
(16) Menahem, T.; Mastai, Y. *J. Polym. Sci., Part A: Polym. Chem.* **2006**, *44*, 3009–3017.
(17) Medina, D. D.; Goldshtein, J.; Margel, S.; Mastai, Y. *Adv. Funct. Mater.* **2007**, *17*, 944–950.
(18) Raman, N. K.; Anderson, M. T.; Brinker, C. J. *Chem. Mater.* **1996**, *8*, 1682–1701.
(19) Alvaro, M.; Benitez, M.; Das, D.; Ferrer, B.; Garcia, H. *Chem. Mater.* **2004**, *16*, 2222–2228.
(20) Baleizao, C.; Gigante, B.; Das, D.; Alvaro, M.; Garcia, H.; Corma, A. *Chem. Commun.* **2003**, *15*, 1860–1861.
(21) Lee, S. B.; Mitchell, D. T.; Trofin, L.; Nevanen, T. K.; Soderlund, H.; Martin, C. R. *Science* **2002**, *296*, 2198–2200.
(22) Fireman-Shoresh, S.; Avnir, D.; Marx, S. *Chem. Mater.* **2003**, *15*, 3607.
(23) Sharon, F.-H.; Sharon, M.; David, A. *Adv. Mater.* **2007**, *19*, 2145–2150.
(24) Lahav, M.; Kharitonov, A. B.; Willner, I. *Chem.—Eur. J.* **2001**, *7*, 3992–3997.
(25) Thomas, A.; Antonietti, M. *Adv. Funct. Mater.* **2003**, *13*, 763–666.
(26) Seddon, A. M.; Patel, H. M.; Burkett, S. L.; Mann, S. *Angew. Chem., Int. Ed.* **2002**, *41*, 2988–2991.
(27) Wang, B.; Chi, C.; Shan, W.; Zhang, Y. H.; Ren, N.; Yang, W. L.; Tang, Y. *Angew. Chem., Int. Ed.* **2006**, *45*, 2088–2090.
(28) Wood, A. *Chem. Week* **2004**, *166*, 27–28.
(29) Che, S.; Liu, Z.; Ohsuna, T.; Sakamoto, K.; Terasaki, O.; Tatsumi, T. *Nature* **2004**, *429*, 281–284.
(30) Polarz, S.; Kuschel, A. *Adv. Mater.* **2006**, *18*, 1206–1209.
(31) Jung, J. H.; Ono, Y.; Hanabusa, K.; Shinkai, S. *J. Am. Chem. Soc.* **2000**, *122*, 5008–5009.
(32) Palmer, C. P.; McCarney, J. P. *J. Chromatogr., A* **2004**, *1044*, 159–171.
(33) Becker, J. J.; Gagne, M. R. *Organometallics* **2003**, *22*, 4984–4998.
(34) Torney, F.; Trewyn, B. G.; Lin, V. S.-Y.; Wang, K. *Nat. Nanotech.* **2007**, *2*, 295–300.
(35) Lee, C. H.; Lo, L. W.; Mou, C. Y.; Yang, C. S. *Adv. Funct. Mater.* **2008**, *18*, 3283–3292.
(36) Kim, H. J.; Lee, S. J.; Park, S. Y.; Jung, J. H.; Kim, J. S. *Adv. Mater.* **2008**, *20*, 3229–3234.
(37) Hu, S.-H.; Liu, T.-Y.; Huang, H.-Y.; Liu, D.-M.; Chen, S.-Y. *Langmuir* **2008**, *24*, 239.
(38) Colfen, H. *Macromol. Rapid Commun.* **2001**, *22*, 219–252.
(39) Schlaad, H.; Antonietti, M. *Eur. Phys. J. E* **2003**, *10*, 17–23.
(40) Sedlak, M. *Czech. Chem. Commun.* **2005**, *70*, 269–291.
(41) Kasparova, P.; Antonietti, M.; Colfen, H. *Eng. Aspects* **2004**, *250*, 153–162.
(42) Harada, M.; Adachi, M. *Adv. Mater.* **2000**, *12*, 839–841.
(43) Deming, T. J. *Nature* **1997**, *390*, 386–389.
(44) Deming, T. J. *Adv. Mater.* **1997**, *9*, 299–311.
(45) Greenfieldi, N.; Fasman, G. D. *Biochemistry* **1969**, *8*, 4108–4116.
(46) Matsuo, K.; Yonehara, R.; Gekko, K. *J. Biochem.* **2004**, *135*, 405–411.

(47) Lavasanifar, A.; Samuel, J.; Kwon, G. S. *Adv. Drug Delivery Rev.* **2002**, *54*, 169–190.
(48) Harada, M.; Adachi, M. *Adv. Mater.* **2000**, *12*, 839–841.
(49) Zhang, Z. M.; Wei, Z. X.; Wan, M. X. *Macromolecules* **2002**, *35*, 5937–5942.
(50) Adachi, M.; Harada, T.; Harada, M. *Langmuir* **2000**, *16*, 2376–2384.
(51) Fuhrhop, J.-H.; Schnieder, P.; Rosenberg, J.; Boekema, E.; Helfrich, W. *J. Am. Chem. Soc.* **1988**, *110*, 2861–2867.
(52) Shimizu, T.; Masuda, M.; Minamikawa, H. *Chem. Rev.* **2005**, *105*, 1401–1443.
(53) Kirchner, R.; Seidel, J.; Wolf, G.; Wulff, G. *J. Phenom. Macrocycl. Chem.* **2002**, *43*, 279–283.
(54) Weber, A.; Dettling, M.; Brunner, H.; Tovar, G. E. M. *Macromol. Rapid Commun.* **2002**, *23*, 824–828.
(55) Dryzun, C.; Mastai, Y.; Shvalb, A.; Avnir, D. *J. Mater. Chem.* **2009**, *19*, 2062–2069.
(56) Eliel, E. L.; Wilen, S. H. *Stereochemistry of Organic Compounds*; Wiley: London, 1994.
(57) Gabashvili, A.; Medina, D. D.; Gedanken, A.; Mastai, Y. *J. Phys. Chem. B* **2007**, *111*, 11105–11110.

AM9003842